Am J Transl Res 2026;18(3):2507-2521
www.ajtr.org /ISSN:1943-8141/AJTR0170154

Original Article

Network pharmacology identifies the mechanisms of action of Jianpi Yanggan Pill in treating diarrhea-predominant irritable bowel syndrome

Ke Ma[1,2*], Xiaokun Hua[3*], Zhipeng Li[4], Shenghua Zhang[5], Ting Zhu[6], Linxi Jin[7], Weiping Li[5], Jingran Shao[8], Xiang Li[8], Weibo Wen[1,8], Yunpeng Luan[8]

[1]First Clinical Medical College, Nanjing University of Chinese Medicine, Nanjing 210023, Jiangsu, China; [2]Department of Pi-wei Diseases, The First Affiliated Hospital of Yunnan University of Chinese Medicine, Kunming 650021, Yunnan, China; [3]Department of Anorectal, Kunming Municipal Hospital of Traditional Chinese Medicine, The Third Affiliated Hospital of Yunnan University of Chinese Medicine, Kunming 650011, Yunnan, China; [4]Yunnan Institute of Product Quality Supervision and Inspection, Kunming 650223, Yunnan, China; [5]Department of Pi-wei Diseases, Affiliated Hospital of Traditional Chinese Medicine of Chongqing Three Gorges Medical College, Chongqing 404606, China; [6]Department of Pi-wei Diseases, Huize County Hospital of Traditional Chinese Medicine, Qujing 650021, Yunnan, China; [7]First Clinical Medical College, Fujian University of Traditional Chinese Medicine, Fuzhou 350108, Fujian, China; [8]The First Affiliated Hospital of Yunnan University of Chinese Medicine, Kunming 650021, Yunnan, China. [*]Equal contributors and co-first authors.

Received November 20, 2025; Accepted February 13, 2026; Epub March 15, 2026; Published March 30, 2026

Abstract: Objective: To investigate the molecular mechanisms of Jianpi Yanggan Pill (JPYGP) in treating Diarrhea-predominant irritable bowel syndrome (IBS-D) using an integrated network pharmacology approach combined with experimental validation. Methods: The chemical constituents of JPYGP were identified by ultra-high performance liquid chromatography-high-resolution mass spectrometry (UHPLC-MS/MS), and bioactive compounds were screened using various databases. Candidate targets was predicted, followed by Gene Ontology (GO) and Kyoto Encyclopedia of Genes and Genomes (KEGG) pathway enrichment studies. An IBS-D rat model was established using acetic acid enema combined with restraint stress. The therapeutic potential of JPYGP was further validated through biochemical assays, including Western blotting and enzyme-linked immunosorbent assay (ELISA), to assess the involvement of the C-X-C motif chemokine ligand 8 and extracellular signal-regulated kinase (CXCL8-ERK) signaling pathway. Results: UHPLC-MS/MS analysis identified 2,309 candidate compounds in JPYGP, among which 20 were bioactive. A total of 660 targets were predicted, of which 414 overlapped with IBS-D-related targets. Enrichment analysis highlighted that these targets were mainly involved in inflammatory and MAPK pathways. In a living organism, JPYGP noticeably alleviated diarrhea symptoms and visceral pain, reduced colonic tissue damage, inhibited mast cell activation, and downregulated the expression of CXCL8 and phosphorylated ERK1/2. Conclusion: JPYGP exerts therapeutic effects on IBS-D via a multi-component, multi-target mechanism, primarily by suppressing the CXCL8-ERK pathway, thereby attenuating colonic inflammation and visceral hypersensitivity.

Keywords: Jianpi Yanggan Pill, diarrhea-predominant irritable bowel syndrome, network pharmacology, CXCL8-ERK signaling pathway, visceral hypersensitivity

Introduction

Diarrhea-predominant irritable bowel syndrome (IBS-D), also known as irritable bowel syndrome (IBS), is a functional gastrointestinal disorder characterized by recurrent abdominal pain or abdominal discomfort associated with altered bowel habits, particularly diarrhea [1]. The etiology and pathogenesis of IBS are not fully understood. Contemporary evidence suggests that IBS-D has multiple factors, including psychosocial stress, dysregulation of the brain-gut axis [2], altered gastrointestinal motility, visceral hypersensitivity [3], and intestinal microbiota imbalance [4]. Among IBS subtypes, IBS-D is the most prevalent worldwide. Although the overall incidence of IBS in China is lower than the developed countries,

https://doi.org/10.62347/GKZD4349

the incidence of IBS-D has been increasing in China with economic development and improvements in living conditions.

Western treatments for IBS-D are primarily symptomatic treatment, including antispasmodics, antidiarrheal agents, gastrointestinal prokinetics, and probiotics [5]. However, these treatments often fail to provide sustained symptom relief and are associated with high relapse, partial efficacy, and long-term medication use, increasing the economic and psychological burdens on patient [6]. According to Traditional Chinese Medicine (TCM), which emphasizes holistic and individualized approach, IBS-D corresponds to the syndrome category of "Xiexie". This therapy has curative efficacy, low cost in the clinic, and good patient acceptance for IBS-D.

Jianping Yanggan Pill (JPYGP), developed by professor Long Zuhong, comprises 14 herbal components: Shanyao (Dioscoreae Rhizoma), Baizhu (Atractylodes macrocephala Koidz), Beishashen (Glehniae Radix), Yinchaihu (Stellariae Radix), Baishao (Paeoniae Radix Alba), Fuling (Poria cocos), Yiyiren (Coicis Semen), Sharen (Amomin Fructus), Wuyao (Linderae Radix), Huangqin (Scutellaria Radix), Wumei (Mume Fructus), Shanzha (Crataegi Fructus), Chenpi (Citri Reticulatae Pericarpium), and Gancao (Glycyrrhizae Radix et Rhizoma). JPYGP, derived from Shenling Baizhu Decoction, is traditionally used to strengthen the spleen and regulate qi. It has been clinically applied to treat spleen and stomach diseases at Yunnan Hospital of Traditional Chinese Medicine, with favorable clinical outcomes. However, the active components, molecular targets, and mechanisms underlying the therapeutic effects of JPYGP in treating IBS-D remain unclear due to the complex composition and multi-herb nature of TCM formulations.

Network pharmacology is a new discipline that integrates systems biology and computer technologies to systematically elucidate drug-component-target-disease interaction networks. This approach enables the comprehensive analysis of how active ingredients modulate disease-related biological networks and is particularly suitable for exploring the multi-component and multi-target characteristics of TCM in the treatment of complex multifactorial diseases. Network pharmacology has been increasingly applied in IBS-D research [7]. In this study, network pharmacology was used to investigate the pharmacological mechanisms of JPYGP in the treatment of IBS-D.

Recent studies have identified C-X-C motif chemokine ligand 8 (CXCL8), also known as interleukin-8 (IL-8), as a key inflammatory mediator involved in IBS-D pathogenesis. CXCL8 enhances neutrophil recruitment and amplifies inflammatory responses. Research reports that elevated CXCL8 in serum and intestinal tissues of IBS-D patient potentially contributes to proinflammatory response and potentiates intestinal dysfunction [8]. CXCL8 mainly exerts its effects through the interaction with CXCR1 and CXCR2 receptors present on the surface of neutrophils, macrophages, and T lymphocytes [9]. In addition, the extracellular signal-regulated kinase 1/2 (ERK 1/2) pathway also plays a critical role in inflammatory regulation by modulating cell proliferation, differentiation, and apoptosis [10, 11]. This study aimed to investigate the effects of JPYGP on CXCL8 expression and ERK1/2 phosphorylation in an IBS-D rat model. Through network pharmacology and *in vivo* experiments, this study sought to elucidate the multi-targeted therapeutic mechanisms of JPYGP in IBS-D management.

Materials and methods

Sample extraction and drug component analysis based on UHPLC-MS/MS

Powdered JPYGP (100 mg, Yunnan Provincial Hospital of TCM) was extracted with 1 mL 70% aqueous methanol. The mixture was vortex-mixed for 30 s followed by water-bath sonication for 90 min. After centrifugation at high speed for 10 min at 4°C, the supernatant was collected and filtered. The filtrate was evaporated to dryness, and the residue was reconstituted in 300 μL of 40% aqueous methanol, vortexed, and centrifuged at 16,000 × g for 10 min at 4°C. The resulting supernatant was subjected to liquid chromatography-mass spectrometry (LC-MS) analysis.

Chromatographic separation was performed using a Vanquish UHPLC system (Thermo Fisher Scientific, Germany) featuring an ACQUITY UPLC HSS T3 column (2.1 × 100 mm; 1.8 μm; Waters). The mobile phases consisted of 0.1% formic acid in water (A) and 0.1% formic acid in acetonitrile (B), with a flow rate of 0.3 mL/min.

Mass spectrometric detection was performed on a Q-Exactive HFX MS (Thermo Fisher Scientific) using electrospray ionization in the positive (3800 V) and negative (3500 V) modes. The sheath gas and auxiliary gas flow rates were set at 45 and 20 arbitrary units, respectively. The ion transfer tube temperature was maintained at 320°C, and the capillary temperature was set at 350°C. Data acquisition was done in Full-MS/dd-MS^2 mode with resolutions of 60,000 and 15,000 over an 90-1,300 m/z range. The top 10 precursor ions were selected for fragmentation using stepped normalized collision energies (NCE) of 20, 40 and 60 eV.

Integrated screening of JPYGP targets and IBS-D-related targets

Targets associated with drug components identified by UHPLC-MS/MS were predicted using the PubChem (https://pubchem.ncbi.nlm.nih.gov/) and SwissTargetPrediction (http://swisstargetprediction.ch/) databases. Then, disease-related targets for IBS-D were retrieved from the GeneCards (https://www.genecards.org/) and Online Mendelian Inheritance in Man (OMIM; https://www.omim.org/) using keyword "Irritable Bowel Syndrome with Predominant Diarrhea". Finally, common targets between JPYGP- and IBS-D-related targets were obtained and visualized using the online Venny 2.1.0 platform.

Construction of a protein-protein interaction (PPI) network and identification of core targets

To elucidate the interactions among the common targets, the intersecting targets screened out in Section 2.2 were imported into the STRING database (https://string-db.org/cgi/input.pl). A high-confidence interaction score (≥0.700) was applied to construct a PPI network, with species set as Homo sapiens. The resulting drug-component-target-disease interaction network depicting the shared genes among the four targets was visualized using Cytoscape 3.10.3, and topological parameters were analyzed using the NetworkAnalyzer. Targets with degree values ≥37 were labeled core targets.

GO and KEGG pathway enrichment analyses

The core targets of JPYGP and IBS-D were imported into the Metascape database (https://metascape.org/) for gene function annotation. The species was set to Homo sapiens, with customized analysis parameters including a minimum overlap of 3, minimum enrichment of 1.5, and *P*-value of 0.05. The top 20 KEGG pathways and the top 10 enriched biological processes (BP), molecular functions (MF), and cellular components (CC) were selected based on statistical significance ($P < 0.05$). Subsequently, visualization of enrichment results was conducted using the online bioinformatics platform (http://www.bioinformatics.com.cn).

Animals

All animal experimental procedures were approved by the Experimental Animal Ethics Committee of Yunnan Provincial Hospital of Traditional Chinese Medicine/The First Affiliated Hospital of Yunnan University (Approval No.: DW-2023-025). Male specific pathogen-free (SPF) Sprague-Dawley rats (8 weeks old) were purchased from SPF (Beijing) Biotechnology Co., Ltd. Rats were housed in a 12-h light/12-h dark cycle with ad libitum access to food and water. Rats were randomly assigned to a control group (n = 8) or subjected to induction of IBS-D.

The animals were restrained using a apparatus that immobilized the limbs while allowing normal breathing and defecation. Animals in IBS-D and JPYGP groups were lightly anesthetized with ether inhalation and injected with 1 ml of 4% acetic acid at a depth of 8 cm from the anus. After 1 min, the colon was flushed with 1 ml phosphate-buffered saline. This procedure was repeated once every other day for a total of two administrations.

Throughout the experimental period, body weight of animals was recorded daily. Fecal samples were collected for diarrhea assessment, and visceral sensitivity was evaluated using the abdominal withdrawal reflex (AWR). The IBS-D model was deemed successfully established when rats exhibited an AWR score ≥3 and a significantly increased diarrhea index was significantly higher compared to the control group. The rats in control group were given normal saline via enema without restrain stress.

Rats with successful model induction were randomly allocated to the IBS-D Model group and the JPYGP group. Rats in the JPYGP group were administered JPYGP orally at 100 mg/kg/day.

On day 21, all animals were euthanized by intraperitoneal injection of tribromoethanol, and biological samples, including blood along with duodenal and colon tissues, were collected for subsequent analyses.

Measurement of AWR scores

Following 12 hours of fasting, a lubricated balloon catheter was inserted 1 cm beyond the anal verge into the colorectum and secured to the tail base with adhesive tape. Rats were acclimatized in a transparent chamber for 30 min. The colorectal distension were carried out at pressures of 20, 40, 60, and 80 mmHg for 20 s at 4 min intervals. The mean AWR scores of three repeated trials were recorded for each pressure. While the inflation of the balloon took place, one experimenter monitored and controlled the pressure parameters, while a second observer, blinded to group allocation, assessed the behavioral responses according to the following criteria: 0, no behavioral changes; 1: no limb movement or simple head movement; 2, abdominal muscle contract; 3: lifting or flattening of the lower abdomen due to strong contraction; 4, pronounced arching of the abdomen accompanied by trunk/pelvis elevation.

Diarrhea index

Rats were housed separately in cages lined with filter paper for fecal collection over a 6-hour period. The index of diarrhea was computed using the following formula:

Diarrhea Index = Loose Stool Rate × Loose Stool Grade

The loose stool rate was calculated by dividing the total number of loose stools by the total number of fecal pellets. Loose stools were identified based on the diameter of fecal contamination on the filter paper and graded as: grade 1, ≤1 cm; grade 2, 1.0-1.9 cm; grade 3, 2.0-3.0 cm; and grade 4, ≥3.0 cm.

Stool trait score

Fecal traits were assessed using the Bristol Stool Form Scale. Stool consistency was classified into seven types as follows: type 1, separate hard lumps resembling nuts; type 2, sausage-shaped but lumpy; type 3, sausage-like with cracks on the surface; type 4, smooth and soft sausage-like or snake-like stool; type 5, soft masses with clear-cut edges; type 6, fluffy pieces with ragged edges, and a mushy paste-like stool; type 7, watery, with no solid components.

Measurement of small intestinal transit

Rats were fasted for 16 h prior to the intestinal transit experiment and then administered 0.2 mL of carbonic ink intragastrically to evaluate small intestinal transit. After 30 min, the rats was euthanized, and the entire intestinal tract was removed from the cardia to the terminal rectum. Without applying tension, the total length of the small intestine and the ink migration distance were measured. The intestinal transit rate was calculated using the following formula:

Ink Propulsion Rate (%) = Ink Migration Distance (cm)/Small Intestine Length (cm) × 100%

Measurement of colonic transit time

Colonic transit time was evaluated using the glass bead expulsion test. Briefly, a lubricated glass bead (3 mm in diameter) was gently inserted 2 cm proximal to the anal verge using a plastic pipette. The distal colonic transit time was defined as the time elapsed between bead insertion and expulsion. Measurements were performed during the final week of the experimental period.

Histopathological grading of the colon

The transverse colon tissues were fixed in 4% neutral buffered formalin, embedded in paraffin, section, and stained with hematoxylin and eosin (H&E) (Leica Biosystems, Germany). Histopathological score was graded as follows: 0, no observable pathological alterations; 1-3, mild injury characterized by slight edema and reduced numbers of mucin-secreting epithelial cells; 4-5, moderate injury with vascular congestion, inflammatory cell infiltration, increased apoptosis and necrosis; and 6-10, severe injury characterized by extensive inflammatory infiltration, marked edema, hemorrhage, vascular congestion, and coagulative necrosis with tissue debris.

Immunofluorescence staining

Paraffin-embedded tissue sections were dewaxed, rehydrated, and treated with a fluorescence quenching agent, rinsed and washed with running water and blocked. Sections were

incubated overnight at 4°C with primary antibody against tryptase (1:500) and subsequently incubated with a fluorescently labeled secondary antibody (1:500) for 1 h at room temperature in the dark. After washing, nuclei were counterstained as appropriate. Immunofluorescence images were captured using a fluorescence microscope (DMi8, Leica Microsystems, Germany), and tryptase-positive mast cells were quantified.

Western blot analysis

Total protein was extracted from colonic tissues using RIPA buffer (Servicebio) containing protease and phosphatase inhibitors. Equal amounts of protein were subjected to SDS-PAGE separation and transferred onto PVDF membranes (Servicebio). After blocking, membranes were incubated overnight at 4°C with rabbit mAbs against ERK1/2 and P-ERK1/2 (1:1000, Servicebio), followed by incubation with HRP-conjugated secondary antibodies (1:10000, Servicebio). Protein bands were visualized with an enhanced chemiluminescence kit (Servicebio) and imaged with an enhanced chemiluminescent detection system (JiaPeng). Band intensity was quantified using ImageJ software.

Data analysis

Statistical analyses were performed using SPSS 27.0 (IBM Corp., Armonk, NY, USA). Data were presented as mean ± standard error of mean. When data followed a normal distribution and met the homogeneity of variance assumption, one-way analysis of variance (ANOVA) was used for comparisons among multiple groups. Subsequent post-hoc testing was performed using Tukey's honestly significant difference (HSD) test to conduct pairwise comparisons between the groups. If the homogeneity of variance assumption was violated, Welch's ANOVA was applied instead, followed by Dunnett's T3 test for post-hoc pairwise comparisons, whereas the Kruskal-Wallis test was applied for non-normally distributed data. A P value < 0.05 was considered statistically significant.

Results

Identification and prediction of active compounds in JPYGP

A total of 2,309 chemical components were identified in JPYGP by UHPLC-MS/MS analysis. High-abundance chromatographic peaks were confirmed based on peak shape and secondary MS fragmentation patterns. Representative total ion chromatograms acquired in both positive and negative ionization modes are shown in **Figure 1A**, **1B**. Of these, 20 active compounds were selected as putative active components for drug target prediction, including 11 flavonoids, four terpenoids, two phenolic acids, one anthraquinone alkaloid, one tyrosine alkaloid, and one small peptide (**Table 1**).

Network pharmacology analysis of JPYGP against IBS-D

Network pharmacology analysis revealed 414 overlapping targets between JPYGP-related and IBS-D-related targets (**Figure 2A**). PPI analysis using STRING database generated a network comprising 400 nodes and 2797 edges. Based on a degree value threshold of ≥37, core targets of JPYGP for treating IBS-D were identified (Dataset S1), and the top 30 targets were selected as core targets (**Figure 2B**).

Among these key core targets, mitogen-activated protein kinases MAPK3 (ERK1) and MAPK1 (ERK2) were prominent, indicating the involvement of the ERK1/2 signaling cascade. GO enrichment analysis demonstrated that these targets were primarily associated with epidermal growth factor receptor (EGFR) signaling-related biological processes and receptor-mediated activation of downstream cascades, including the ERK1/2 pathway. Most targets were localized in the cytoplasm, consistent with their roles in intracellular signal transduction. Molecular function analysis further revealed significant enrichment in protein tyrosine kinase activity, indicating modulation of phosphorylation events that is critical for ERK1/2 activation (**Figure 2C**). KEGG pathway enrichment analysis showed significant overrepresentation of MAPK signaling pathway, supporting a potential role of ERK1/2 in the therapeutic effects of JPYGP in IBS-D (**Figure 2D**).

Therapeutic effects of JPYGP on stress-induced IBS-D

In the IBS-D model induced by restraint stress and acetic acid enema (4%, 10 ml), body weight gain was significantly reduced in both the

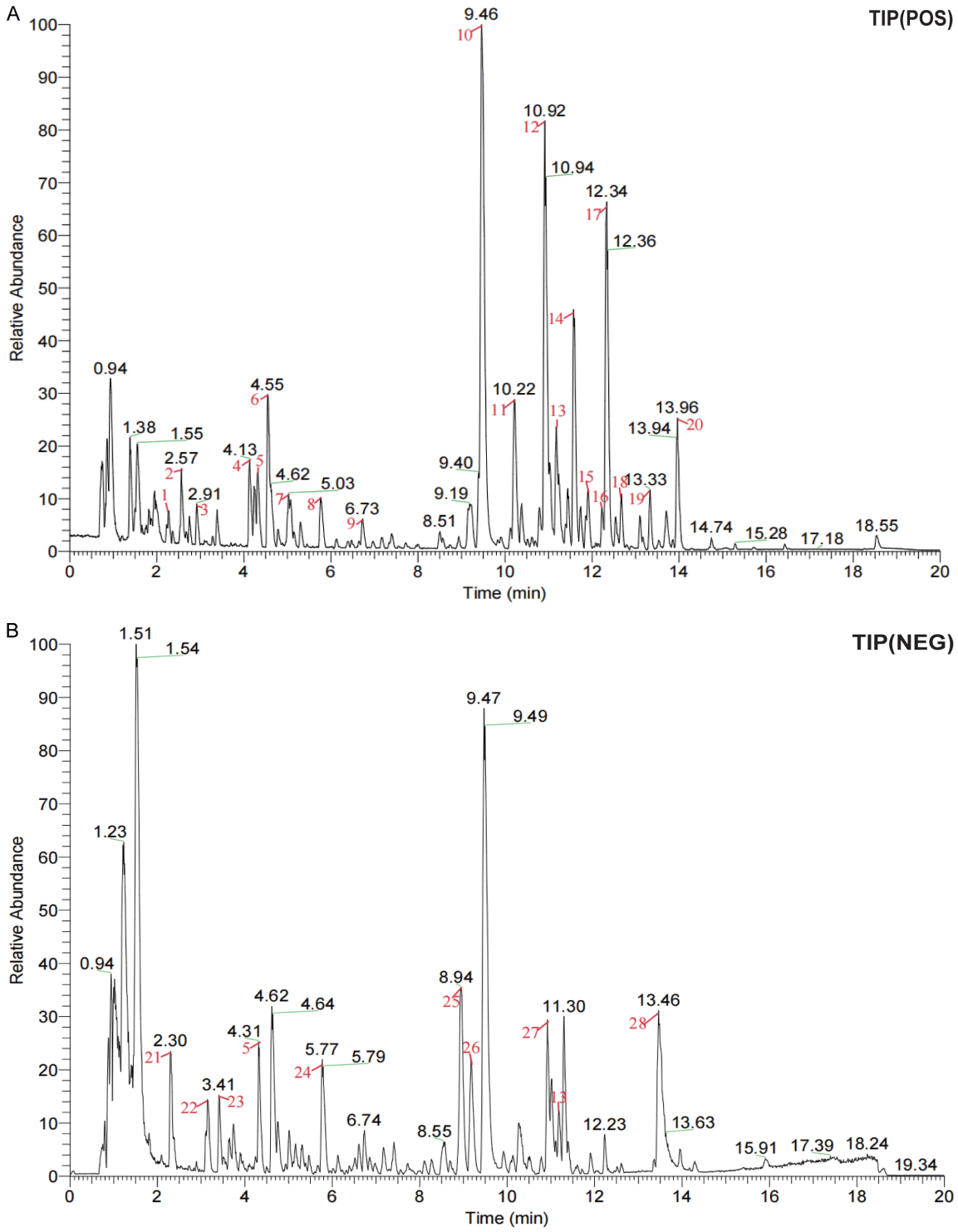

Figure 1. Identification of active compounds in JPYGP using UHPLC-MS/MS. A. Total ion chromatogram of JPYGP in POS mode. B. Total ion chromatogram of JPYGP in NEG mode. JPYGP, Jianpi Yanggan Pill; NEG, negative; POS, positive; UHPLC-MS/MS, ultra-high-performance liquid chromatography-high-resolution mass spectrometry.

model and JPYGP group compared with the control group. After two weeks of treatment, rats in the JPYGP group experienced greater weight recovery than the model group, although

Table 1. Chemical characterization of bioactive compounds in Jianpi Yanggan Pill (JPYGP)

NO.	Name	Formula	RT/ min	m/Z	Ion Mode
2	Valylphenylalanine	C14H20N2O3	2.58	166.0862	POS
4	(R)-Reticuline	C19H23NO4	4.14	330.1696	POS
5	Albiflorin	C23H28O11	4.32	481.1701	POS/NEG
9	Axillarin 4'-glucuronide	C23H22O14	6.73	347.0758	POS
10	Baicalein	C15H10O5	9.47	271.0596	POS
11	Sinensetin	C20H20O7	10.23	373.1278	POS
12	Nobiletin	C21H22O8	10.92	403.1383	POS
13	Oroxylin	C16H12O5	11.19	285.0747	POS/NEG
14	Tangerlin	C20H20O7	11.59	373.1278	POS
15	1-(3,4-Dihydroxy-2,6-dimethoxyphenyl)-3-phenylprop-2-en-1-one	C17H16O5	11.91	301.1068	POS
16	Ligustilide A	C12H14O2	12.24	191.1066	POS
18	Atractylenolide II	C15H20O2	12.68	233.1535	POS
19	Atractylenolide I	C15H18O2	13.33	231.1379	POS
20	(-)-Isolongifolol	C15H26O	13.96	205.1945	POS
21	Ethyl gallate	C9H10O5	2.35	169.0135	NEG
22	3,4-Dihydroxybenzoic acid	C7H6O4	3.18	153.0182	NEG
24	Hesperidin	C28H34O15	5.8	609.1817	NEG
25	Naringin	C27H32O14	8.96	271.061	NEG
26	Norwogenin	C15H10O5	9.19	269.0455	NEG
27	Wogonin	C16H12O5	10.93	283.0609	NEG

body weight remained lower than that of the control group ($P < 0.05$ or $P< 0.01$; **Figure 3A**). AWR scores, an indicator of visceral sensitivity, increased progressively with colorectal distension pressure in the model group compared with controls, whereas AWR scores were significantly reduced in the JPYGP group ($P < 0.05$ or $P < 0.01$; **Figure 3B**). The diarrhea index in JPYGP group was markedly decreased compared with the model group ($P < 0.001$; **Figure 3C**). Consistently, Bristol stool scores in JPYGP group were significantly lower than that in the model group ($P < 0.001$), suggesting that JPYGP not only alleviated diarrhea severity but also improved stool consistency (**Figure 3D**).

Effects of JPYGP on gastrointestinal motility in IBS-D rats

Gastrointestinal motility was assessed by measuring intestinal transit. The small intestine propulsion rates in both model and JPYGP groups were significantly higher than those in the control group. Noteworthy, the propulsion rate in the JPYGP group was significantly lower than that in the model group ($P < 0.001$; **Figure 4A**). In the glass bead expulsion test, the model group demonstrated significantly shorter colonic transit time compared with the control group ($P < 0.05$), while colonic transit time was prolonged in the JPYGP group compared with the model group ($P < 0.01$; **Figure 4B**). Furthermore, carbon ink was predominantly distributed in the small intestine all groups at 30 min after gavage (**Figure 4C**).

JPYGP attenuated colonic inflammation and suppresses mast cell activation

Histopathological examination of colonic tissues using H&E staining revealed that rats in the control group exhibited intact colonic mucosal structure with clearly visible goblet cells. In contrast, rats in the IBS-D group showed significant crypt destruction, mucosal ulceration, and extensive inflammatory cell infiltration, with a pathological score of 4.

Administration of JPYGP markedly reduced histopathological alterations, with a pathological score decreased to 2 (**Figure 5A**, **5B**). To further assess the involvement of mast cells in IBS-D pathology, immunofluorescence staining for tryptase-positive mast cells was performed. Results showed a marked increase in tryptase-positive mast cells (red) in the model tissues as compared with controls, which was notably reduced after JPYGP treatment. Nuclear counterstaining with DAPI (blue) revealed preserved

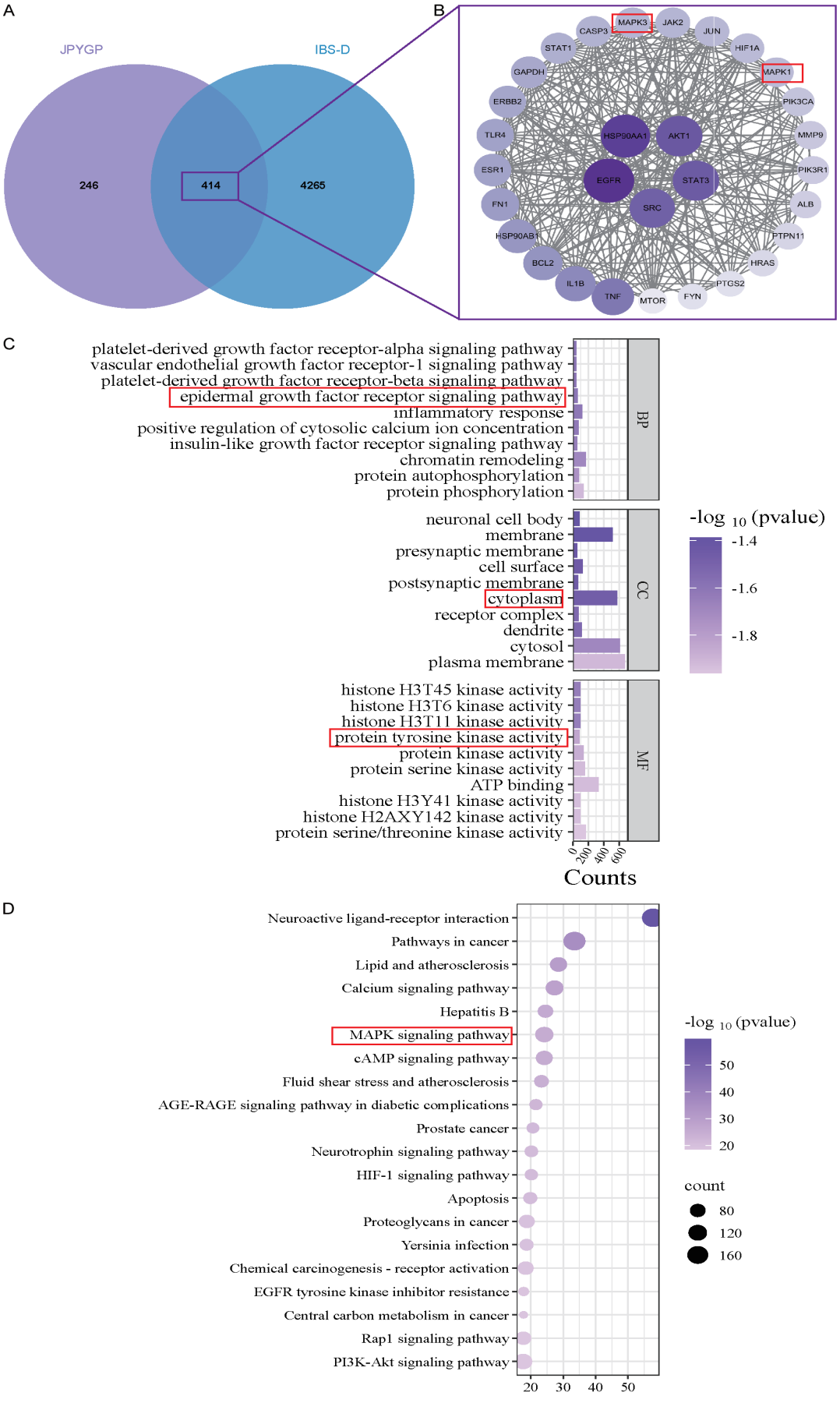
A
JPYGP
IBS-D
246
414
4265
B
MAPK3
JAK2
CASP3
JUN
STAT1
HIF1A
GAPDH
MAPK1
ERBB2
PIK3CA
TLR4
HSP90AA1
AKT1
MMP9
ESR1
EGFR
STAT3
PIK3R1
FN1
SRC
ALB
HSP90AB1
PTPN11
BCL2
HRAS
IL1B
PTGS2
TNF
MTOR
FYN
C
platelet-derived growth factor receptor-alpha signaling pathway
vascular endothelial growth factor receptor-1 signaling pathway
platelet-derived growth factor receptor-beta signaling pathway
epidermal growth factor receptor signaling pathway
inflammatory response
positive regulation of cytosolic calcium ion concentration
insulin-like growth factor receptor signaling pathway
chromatin remodeling
protein autophosphorylation
protein phosphorylation
BP
neuronal cell body
membrane
presynaptic membrane
cell surface
postsynaptic membrane
cytoplasm
receptor complex
dendrite
cytosol
plasma membrane
CC
histone H3T45 kinase activity
histone H3T6 kinase activity
histone H3T11 kinase activity
protein tyrosine kinase activity
protein kinase activity
protein serine kinase activity
ATP binding
histone H3Y41 kinase activity
histone H2AXY142 kinase activity
protein serine/threonine kinase activity
MF
0
200
400
600
Counts
-log 10 (pvalue)
-1.4
-1.6
-1.8
D
Neuroactive ligand-receptor interaction
Pathways in cancer
Lipid and atherosclerosis
Calcium signaling pathway
Hepatitis B
MAPK signaling pathway
cAMP signaling pathway
Fluid shear stress and atherosclerosis
AGE-RAGE signaling pathway in diabetic complications
Prostate cancer
Neurotrophin signaling pathway
HIF-1 signaling pathway
Apoptosis
Proteoglycans in cancer
Yersinia infection
Chemical carcinogenesis - receptor activation
EGFR tyrosine kinase inhibitor resistance
Central carbon metabolism in cancer
Rap1 signaling pathway
PI3K-Akt signaling pathway
20
30
40
50
-log 10 (pvalue)
50
40
30
20
count
80
120
160

Figure 2. Network pharmacology analysis of JPYGP against IBS-D. A. Venn diagram showing 414 overlapping targets between JPYGP compounds and IBS-D. B. PPI network of JPYGP targets for the treatment of IBS-D, consisting of 400 nodes and 2797 edges (top 30 core targets highlighted). C. GO analysis of JPYGP targets in IBS-D (top 10). D. KEGG enrichment analysis of JPYGP targets in IBS-D (top 20). GO, Gene Ontology; IBS-D, diarrhea-predominant irritable bowel syndrome; JPYGP, Jianpi Yanggan Pill; KEGG, Kyoto Encyclopedia; PPI, protein-protein interaction.

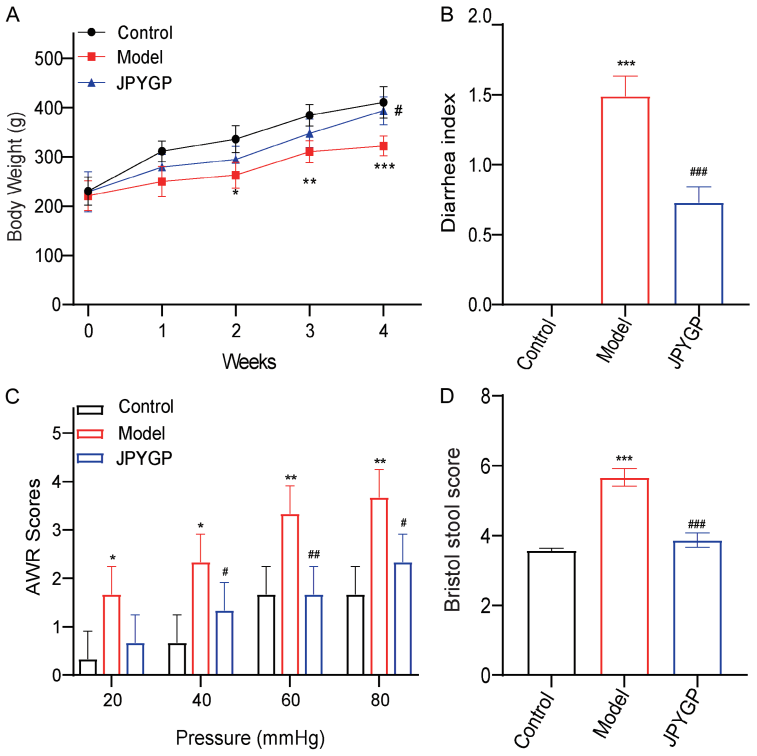

Figure 3. Therapeutic effects of JPYGP on stress-induced IBS-D. A. Changes in body weight over the 4-week experimental period. B. Diarrhea index of rats in each group. C. Abdominal withdrawal reflex (AWR) scores in response to colorectal distension at different pressures (20, 40, 60, and 80 mmHg). D. Bristol stool scores evaluating stool consistency. Data are presented as the mean ± SEM (n = 8). $^{*}P < 0.05$, $^{**}P < 0.01$, $^{***}P < 0.001$ vs. Control group; $^{\#}P < 0.05$, $^{\#\#}P < 0.01$, $^{\#\#\#}P < 0.001$ vs. Model group. AWR, abdominal withdrawal reflex; IBS-D, diarrhea-predominant irritable bowel syndrome; JPYGP, Jianpi Yanggan Pill; ns, no significance; SEM, standard error of the mean.

tissue architecture (**Figure 5C**). Quantitative analysis confirmed significantly increased number of tryptase-positive mast cells in the model group and significant decreased number after JPYGP treatment (**Figure 5D**), indicating that JPYGP effectively attenuated colonic inflammation and mast cell activation in IBS-D rats.

JPYGP reduced CXCL8 expression and inhibited ERK pathway activation in serum and colonic mucosa

To evaluate inflammatory responses and signaling mechanism in IBS-D rat model, levels of the pro-inflammatory chemokine CXCL8 and activation of the ERK1/2 pathway were assessed. Serum and colonic mucosal samples were collected for ELISA to quantify CXCL8 expression, and western blot was performed to determine ERK1/2 phosphorylation. CXCL8 expression in serum and colonic mucosal tissues was significantly elevated in the IBS-D model than in the control group ($P < 0.001$), but their levels were significantly reduced after JPYGP treatment ($P < 0.001$) (**Figure 6A**, **6B**). Consistently, ERK1/2 phosphorylation in colon tissues was markedly increased in the model group ($P < 0.001$), confirming activation of the ERK pathway (**Figure 6C-E**). JPYGP treatment significantly mitigated suppressed ERK1/2 phosphorylation ($P < 0.001$) (**Figure 6F**). These findings suggest that JPYGP exerts anti-inflammatory and therapeutic effects in IBS-D, at least in part, through inhibition of the CXCL8-ERK signaling pathway.

Discussion

IBS-D is a common functional gastrointestinal disorder, and current Western medical management primarily focuses on symptom control [12]. Nonetheless, this approach has its drawbacks, including side effects and high relapse rates after drug discontinuation [13-15]. In comparison, TCM emphasizes holistic regulation and multi-target intervention, offering a distinct conceptual framework for IBS-D management [16, 17]. In this study, network pharmacology combined with *in vivo* experiments was employed to elucidate the underlying mechanisms of JPYGP, a Chinese herbal formula that harmonizes the liver and spleen, acting through multiple components, targets, and pathways.

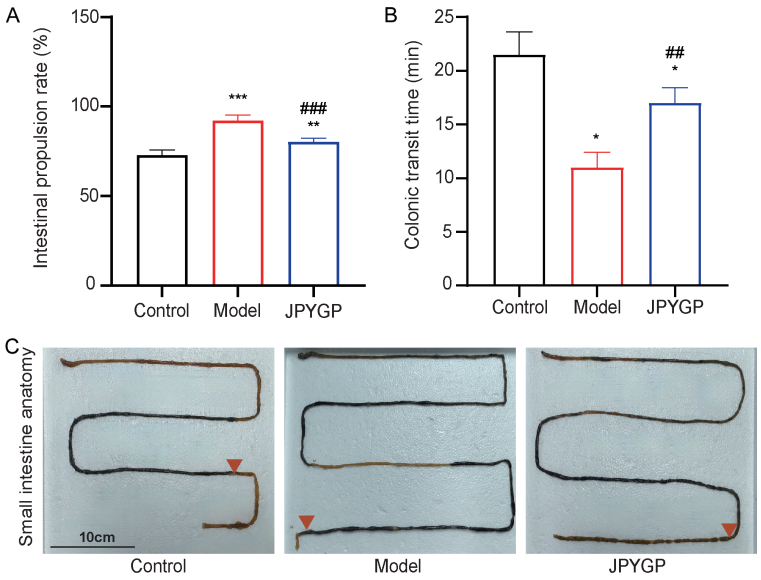

Figure 4. Effect of JPYGP on gastrointestinal motility in IBS-D rats. A. Small intestinal propulsion rate. B. Colonic transit time. C. Representative gross images of the small intestine showing the distance of carbon ink migration (indicated by red arrowheads). Data are presented as the mean ± SEM (n = 8). *P < 0.05, **P < 0.01, ***P < 0.001 vs. Control group; ##P < 0.01, ###P < 0.001 vs. Model group. IBS-D, diarrhea-predominant irritable bowel syndrome; JPYGP, Jianpi Yanggan Pill; ns, no significance; SEM, standard error of the mean.

IBS-D is no longer considered merely a disorder of gastrointestinal motility. Increasing evidence shows that it is driven by a complex interplay of factors, including immune-inflammatory activation and brain-gut axis dysregulation [18]. For instance, network pharmacology combined with cellular experiments has confirmed that TCM compounds can exert therapeutic effects by inhibiting the MAPK signaling pathway, including downstream targets such as ERK and JNK, and down-regulating other key inflammatory factors IL-6, TNF, and CXCL8 [19]. These findings indicate that aberration activation of the MAPK pathway and excessive release of inflammatory factors play crucial roles in the pathogenesis of IBS-D. Furthermore, activation of the ERK1/2 pathway in intestinal dendritic cells of IBS model rats has been shown to be closely linked to their aberrant immune phenotypes and enhanced visceral hypersensitivity [20]. Activated immune cells, particularly mast cells, release mediators that facilitate nociceptive nerve sensitization, thereby contributing to abdominal pain. In addition, patients with visceral hypersensitivity often exhibit impaired intestinal barrier function and low-grade immune activation, forming a vicious cycle [21].

This study demonstrated, through network pharmacology and *in vivo* experiments, that JPYGP may exert therapeutic effects on IBS-D by acting on multiple targets and pathways. UHPLC-MS/MS analysis of JPYGP identified a total of 2,309 chemical constituents, from which 20 potential active compounds were screened. These compounds collectively predicted a total of 660 putative targets, of which 414 overlapped with IBS-D-related targets. GO functional enrichment analysis revealed 1714 BPs, 172 CCs, and 228 MFs, and KEGG pathway enrichment analysis identified 211 associated signaling pathways. These findings highlight the multi-component, multi-target, and multi-pathway therapeutic characteristics of TCM formulas. Consistently, *in vivo* experiments further demonstrated that JPYGP significantly alleviated diarrhea symptoms in IBS-D rats, reduced AWR scores, mitigated colonic tissue injury, inhibited CXCL8 expression, and downregulated ERK1/2 phosphorylation.

CXCL8 was the first chemokine to be purified and sequenced and was recognized as a neutrophil-activating factor secreted by the human monocyte-macrophage system. It has been shown to induce neutrophil exocytosis, promote the production of superoxide and hydrogen peroxide, resist serum-mediated inactivation, and accumulate at sites of inflammation [22, 23]. CXCL8 is a 72-amino-acid CXC chemokine characterized by three antiparallel β-strands and a C-terminal α-helix (residues 57-72). Its tertiary structure is stabilized by two disulfide bonds (Cys7-Cys34 and Cys9-Cys50), separated by a glutamine residue (Gln8) between Cys7 and Cys9 [24]. Research has shown that CXCL8 is highly expressed in colorectal carcinoma, with elevated levels correlating with advanced disease stage and poor prognosis, supporting its pro-tumorigenic and pro-inflammatory role rather than a protective function [25, 26]. In gastrointestinal diseases,

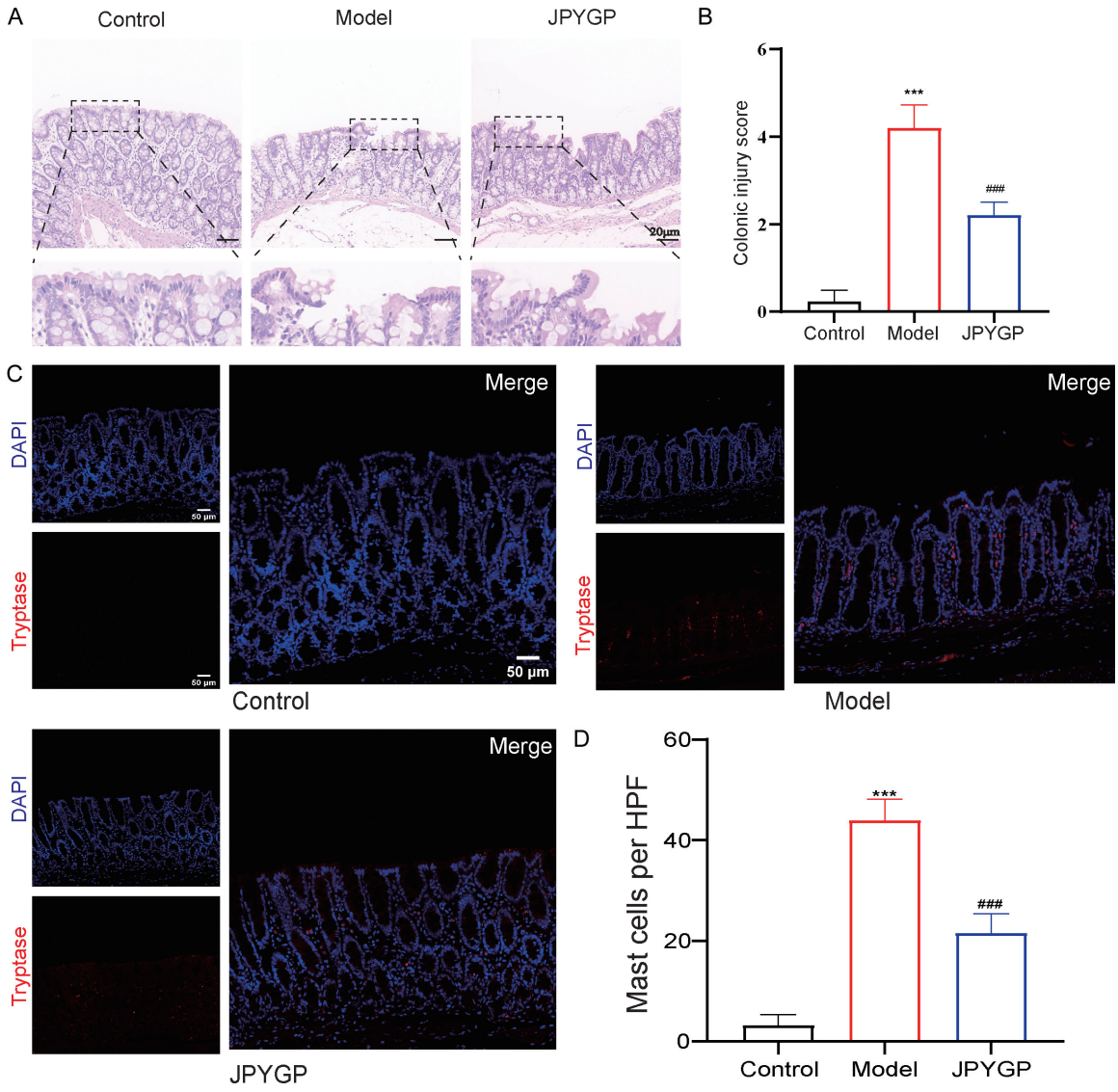

Figure 5. Effects of JPYGP on colonic histopathology and mast cell activation in IBS-D rats. A. Representative H&E staining of colonic tissues. The lower panels represent magnified views of the boxed areas in the upper panels. Scale bar = 20 μm. B. Histopathological injury scores of colonic tissues. C. Representative immunofluorescence staining for tryptase (red, marking mast cells) and DAPI (blue, marking nuclei). Scale bar = 50 μm. D. Quantification of tryptase-positive mast cells per high-power field (HPF). Data are presented as the mean ± SEM. $^{***}P < 0.001$ vs. Control group; $^{###}P < 0.001$ vs. Model group. DAPI, 4',6-diamidino-2-phenylindole; H&E, hematoxylin and eosin; IBS-D, diarrhea-predominant irritable bowel syndrome; JPYGP, Jianpi Yanggan Pill.

the CXCL8-CXCR1/2 axis plays an instrumental role in neutrophil recruitment, immune activation, and pain sensitization [27, 28]. The occurrence of low-grade immune activation in IBS-D, indicated by an increase in mucosal mast cells, T-cell infiltration, and higher pro-inflammatory cytokine levels, is implicated in visceral hypersensitivity and altered gut motility [29, 30]. As per our data, expression of CXCL8 and its receptors (CXCR1/CXCR2) was upregulated in colon tissues of IBS-D model rats. Previous studies have similarly shown that CXCL8 is upregulated in IBS-D patients. Enhanced activation of the CXCL8-CXCR1/2 pathway can further stimulate downstream signaling cascades, including PI3K/Akt, MAPK, and NF-κB, pathways, thereby aggravating inflammation and visceral pain [31, 32].

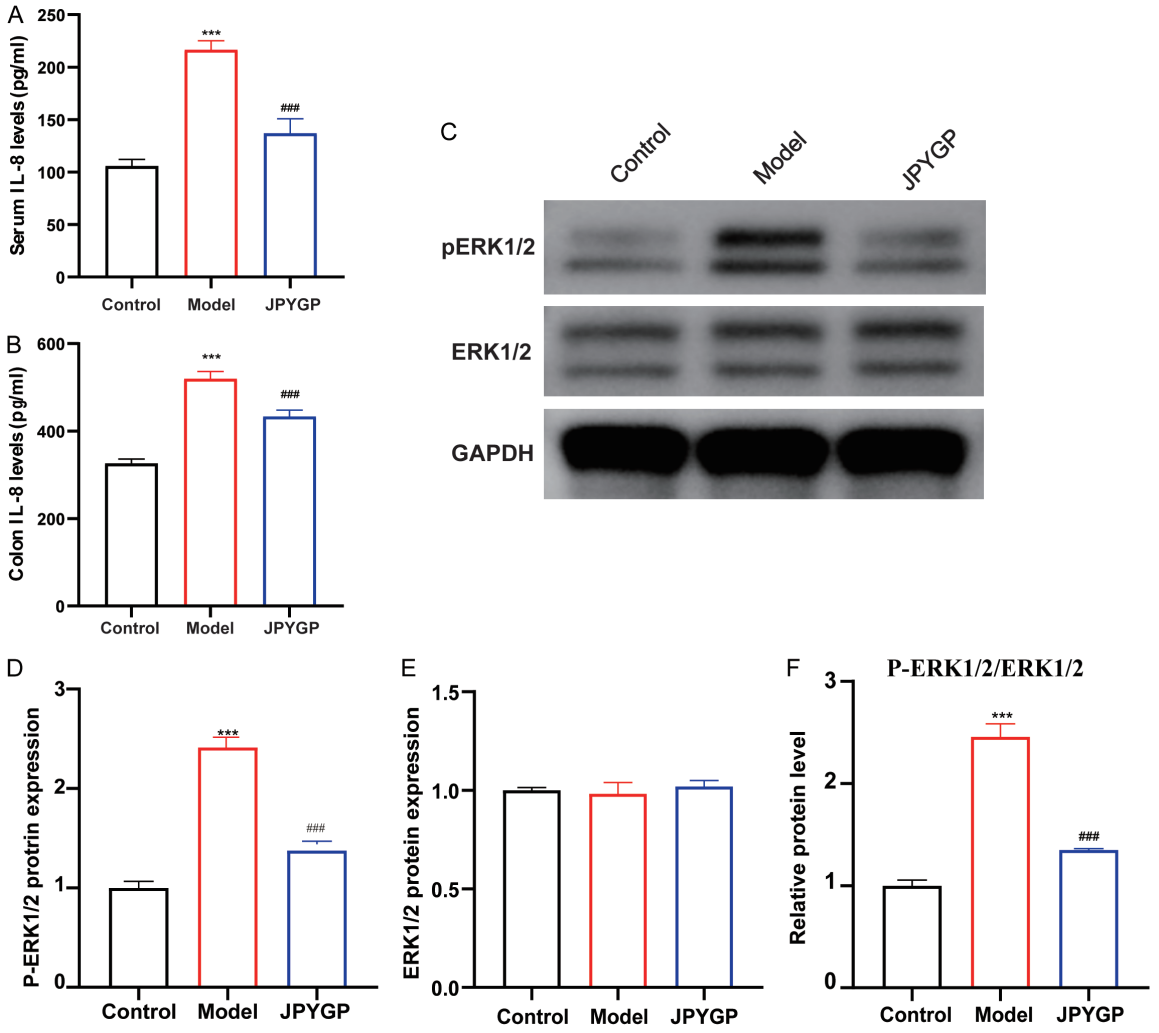

Figure 6. Influence of JPYGP on CXCL8 expression and the ERK1/2 signaling pathway in IBS-D rats. A. Serum levels of CXCL8 (labeled as IL-8). B. Colonic tissue levels of CXCL8 (labeled as IL-8). C. Representative Western blot bands showing the expression of p-ERK1/2, total ERK1/2, and GAPDH (internal control). D. Quantitative analysis of p-ERK1/2 protein expression relative to GAPDH. E. Quantitative analysis of total ERK1/2 protein expression relative to GAPDH. F. The ratio of p-ERK1/2 to total ERK1/2 protein expression. Data are presented as the mean ± SEM (n = 8). $^{***}P < 0.001$ vs. Control group; $^{###}P < 0.001$ vs. Model group. CXCL8, C-X-C motif chemokine ligand 8; ERK, extracellular signal-regulated kinase; GAPDH, glyceraldehyde-3-phosphate dehydrogenase; IL-8, interleukin-8; IBS-D, diarrhea-predominant irritable bowel syndrome; JPYGP, Jianpi Yanggan Pill.

In this study, the potential mechanisms by which JPYGP exerts therapeutic effects against IBS-D were investigated using network pharmacology and UHPLC-MS/MS to identify active ingredients. The major compounds, including flavonoids, terpenoids, phenolic acids, anthraquinone alkaloids and tyrosine alkaloid, have been widely reported to possess anti-inflammatory and intestinal-protective activities, providing chemical basis supporting the observed downregulation of CXCL8 expression and inhibition of ERK1/2 phosphorylation. Previous studies have demonstrated that flavonoids can suppress pro-inflammatory gene expression, enhance anti-inflammatory signals like IL-10, and stabilize intestinal barrier by modulating small intestine and colonic macrophages (AhR-dependent manner), thereby reducing visceral hypersensitivity and diarrhea-associated pathology [34]. Evidence suggests that orally administered terpenoids (e.g., thymol) may ameliorate stress-induced IBS phenotypes, including intestinal hypermotility/dysmotility and visceral hypersensitivity [35, 36]. Phenolic acids have also been reported to mitigate diarrhea, visceral pain sensitivity, and intestinal barrier disrup-

tion in IBS animal models [37, 38]. Collectively, these findings indicate that the therapeutic efficacy of JPYGP is mediated through coordinated regulation of immune-related components and multiple signaling pathways, consistent with the multi-target and system-level regulatory characteristics of traditional Chinese medicine.

Conclusions

JPYGP can modulate key inflammatory signaling pathways in IBS-D, with particular emphasis on suppression of the CXCL8-CXCR1/2-ERK axis, thereby alleviating diarrhea, visceral hypersensitivity, and colonic inflammation. These findings provide a scientific rationale for the clinical application of JPYGP in TCM and support its potential as a multi-target therapeutic agent for IBS-D. Future investigations should focus on isolating and validating individual active constituents to confirm their direct molecular interactions through *in vitro* experiments and clinical investigations.

Acknowledgements

We would like to express our appreciation to the Central Laboratory of Yunnan Provincial Hospital of Traditional Chinese Medicine and Yunnan Provincial Engineering Research Center for their strong support in completing this study. This study was supported through the Joint Special Project of Traditional Chinese Medicine by the Yunnan Provincial Science and Technology Department (Grant No. 202101AZ07-0001-233, 202301AZ070001-024).

Disclosure of conflict of interest

None.

Abbreviations

IBS-D, Diarrhea-predominant irritable bowel syndrome; JPYGP, Jianpi Yanggan Pill; CXCL8, C-X-C motif chemokine ligand 8; ERK, Extracellular signal-regulated kinase; P-ERK, Phosphorylated extracellular signal-regulated kinase; PPI, Protein-Protein Interaction; AWR, Abdominal withdrawal reflex; MAPK, Mitogen-activated protein kinase.

Address correspondence to: Yunpeng Luan, The First Affiliated Hospital of Yunnan University of Chinese Medicine, No. 120, Guanghua Street, Kunming 650021, Yunnan, China. Tel: +86-0871-63620626; E-mail: LuanTeam@163.com; Weibo Wen, First Clinical Medical College, Nanjing University of Chinese Medicine, No. 138, Xianlin Avenue, Qixia District, Nanjing 210023, Jiangsu, China. Tel: +86-0871-63620626; E-mail: WeiboWen20-251117@163.com

References

[1] Ford AC, Lacy BE and Talley NJ. Irritable bowel syndrome. N Engl J Med 2017; 376: 2566-2578.
[2] Mayer EA, Tillisch K and Gupta A. Gut/brain axis and the microbiota. J Clin Invest 2015; 125: 926-38.
[3] Saha L. Irritable bowel syndrome: pathogenesis, diagnosis, treatment, and evidence-based medicine. World J Gastroenterol 2014; 20: 6759-73.
[4] Pimentel M and Lembo A. Microbiome and its role in irritable bowel syndrome. Dig Dis Sci 2020; 65: 829-839.
[5] Altomare A, Di Rosa C, Imperia E, Emerenziani S, Cicala M and Guarino MPL. Diarrhea predominant-irritable bowel syndrome (IBS-D): effects of different nutritional patterns on intestinal dysbiosis and symptoms. Nutrients 2021; 13: 1506.
[6] Fliegner-Baia M, Keller J and Layer P. Proper patient counseling, recommended nutrition, specific medication. The basics of irritable bowel syndrome therapy. MMW Fortschr Med 2002; 144: 33-7.
[7] Zhang R, Zhu X, Bai H and Ning K. Network pharmacology databases for traditional chinese medicine: review and assessment. Front Pharmacol 2019; 10: 123.
[8] Seyedmirzaee S, Hayatbakhsh MM, Ahmadi B, Baniasadi N, Bagheri Rafsanjani AM, Nikpoor AR and Mohammadi M. Serum immune biomarkers in irritable bowel syndrome. Clin Res Hepatol Gastroenterol 2016; 40: 631-637.
[9] Mearin F, Ciriza C, Mínguez M, Rey E, Mascort JJ, Peña E, Cañones P and Júdez J. Clinical practice guideline: irritable bowel syndrome with constipation and functional constipation in the adult. Rev Esp Enferm Dig 2016; 108: 332-63.
[10] Enck P, Aziz Q, Barbara G, Farmer AD, Fukudo S, Mayer EA, Niesler B, Quigley EM, Rajilić-Stojanović M, Schemann M, Schwille-Kiuntke J, Simren M, Zipfel S and Spiller RC. Irritable bowel syndrome. Nat Rev Dis Primers 2016; 2: 16014.
[11] Kong T, Liu M, Ji B, Bai B, Cheng B and Wang C. Role of the extracellular signal-regulated Ki-

nase 1/2 signaling pathway in ischemia-reperfusion injury. Front Physiol 2019; 10: 1038.
[12] Staudacher HM, Black CJ, Teasdale SB, Mikocka-Walus A and Keefer L. Irritable bowel syndrome and mental health comorbidity - approach to multidisciplinary management. Nat Rev Gastroenterol Hepatol 2023; 20: 582-596.
[13] Zhou Y, Yang Z, Liu S, Xie S, Zhang Q, Zhang S, Zhu S and Wu S. Long-term risk of irritable bowel syndrome associated with MASLD, MASLD type and different cardiometabolic risk factors: a large-scale prospective cohort study. BMC Gastroenterol 2025; 25: 576.
[14] Chen D, Ni D and Yang H. Combination therapy with otilonium bromide and trimebutine maleate demonstrates significant clinical advantages in irritable bowel syndrome patients. Am J Transl Res 2025; 17: 4859-4866.
[15] Akbari R, Salimi Y, Dehghani-Aarani F and Rezayat E. Attention in irritable bowel syndrome: a systematic review of affected domains and brain-gut axis interactions. J Psychosom Res 2025; 191: 112067.
[16] Zhang S, Tian D, Xia Z, Yang F, Chen Y, Yao Z, He Y, Miao X, Zhou G, Yao X and Tang J. Chang-Kang-Fang alleviates diarrhea predominant irritable bowel syndrome (IBS-D) through inhibiting TLR4/NF-κB/NLRP3 pathway. J Ethnopharmacol 2024; 330: 118236.
[17] Zhang Y, Huang S, Zhang S, Hao Z and Shen J. Pomegranate Peel extract mitigates diarrhea-predominant irritable bowel syndromes via MAPK and NF-κB pathway modulation in rats. Nutrients 2024; 16: 3854.
[18] Aggeletopoulou I, Papantoniou K, Pastras P and Triantos C. Unraveling the pathophysiology of irritable bowel syndrome: mechanisms and insights. Int J Mol Sci 2025; 26: 10598.
[19] Zhang C, Li X, Gao D, Zhu H, Wang S, Tan B and Yang A. Network pharmacology and experimental validation of the anti-inflammatory effect of Tingli Dazao Xiefei decoction in acute lung injury treatment. J Inflamm Res 2023; 16: 6195-6209.
[20] Chen X, Luo Q, Yan X, Li W and Chen S. Vagal transient receptor potential Ankyrin 1 mediates stress-exacerbated visceral mechanonociception after antral cold exposure. J Neurogastroenterol Motil 2019; 25: 442-460.
[21] Hussein H, Van Remoortel S and Boeckxstaens GE. Irritable bowel syndrome: when food is a pain in the gut. Immunol Rev 2024; 326: 102-116.
[22] Peveri P, Walz A, Dewald B and Baggiolini M. A novel neutrophil-activating factor produced by human mononuclear phagocytes. J Exp Med 1988; 167: 1547-1559.
[23] Coperchini F, Chiovato L, Croce L, Magri F and Rotondi M. The cytokine storm in COVID-19: an overview of the involvement of the chemokine/chemokine-receptor system. Cytokine Growth Factor Rev 2020; 53: 25-32.
[24] Cambier S, Gouwy M and Proost P. The chemokines CXCL8 and CXCL12: molecular and functional properties, role in disease and efforts towards pharmacological intervention. Cell Mol Immunol 2023; 20: 217-251.
[25] Łukaszewicz-Zając M, Pączek S, Mroczko P and Kulczyńska-Przybik A. The significance of CXCL1 and CXCL8 as well as their specific receptors in colorectal cancer. Cancer Manag Res 2020; 12: 8435-8443.
[26] Xiao YC, Yang ZB, Cheng XS, Fang XB, Shen T, Xia CF, Liu P, Qian HH, Sun B, Yin ZF and Li YF. CXCL8, overexpressed in colorectal cancer, enhances the resistance of colorectal cancer cells to anoikis. Cancer Lett 2015; 361: 22-32.
[27] Wang P, Yang GL, He YF, Shen YH, Hao XH, Liu HP, Shen HB, Wang L and Sha W. Single-cell transcriptomics of blood identified IFIT1+ neutrophil subcluster expansion in NTM-PD patients. Int Immunopharmacol 2024; 137: 112412.
[28] Qin R, Ren W, Ya G, Wang B, He J, Ren S, Jiang L and Zhao S. Role of chemokines in the crosstalk between tumor and tumor-associated macrophages. Clin Exp Med 2023; 23: 1359-1373.
[29] Gao J, Xiong T, Grabauskas G and Owyang C. Mucosal serotonin reuptake transporter expression in irritable bowel syndrome is modulated by gut microbiota via mast cell-prostaglandin E2. Gastroenterology 2022; 162: 1962-1974, e6.
[30] Wu BY, Xu P, Cheng L, Wang QQ, Qiu HY, Yan XJ and Chen SL. The alteration of mucosal bile acid profile is associated with nerve growth factor expression in mast cells and bowel symptoms in diarrhea-predominant irritable bowel syndrome. Clin Exp Immunol 2024; 216: 200-210.
[31] Shen S, Fu B, Deng L, Zhu G, Shi H, Tian G, Han C, Yi P and Peng L. Paeoniflorin protects chicken against APEC-induced acute lung injury by affecting the endocannabinoid system and inhibiting the PI3K/AKT and NF-κB signaling pathways. Poult Sci 2024; 103: 103866.
[32] Yang Q, Guo H, Li H, Li Z, Ni F, Wen Z, Liu K, Kong H and Wei W. The CXCL8/MAPK/hnRNP-K axis enables susceptibility to infection by EV-D68, rhinovirus, and influenza virus in vitro. Nat Commun 2025; 16: 1715.
[33] Qin HY, Zang KH, Zuo X, Wu XA and Bian ZX. Quercetin attenuates visceral hypersensitivity and 5-hydroxytryptamine availability in postinflammatory irritable bowel syndrome rats: role of enterochromaffin cells in the colon. J Med Food 2019; 22: 663-671.

[34] Xu X, Dong Q, Zhong Q, Xiu W, Chen Q, Wang J and Zhou Z. The flavonoid kurarinone regulates macrophage functions via aryl hydrocarbon receptor and alleviates intestinal inflammation in irritable bowel syndrome. J Inflamm Res 2021; 14: 4347-4359.

[35] Subramaniyam S, Yang S, Diallo BN, Fanshu X, Lei L, Li C, Tastan Bishop Ö and Bhattacharyya S. Oral Phyto-thymol ameliorates the stress induced IBS symptoms. Sci Rep 2020; 10: 13900.

[36] Liu F, Shen Y, Li J, Bi L, Ye X, Li Y and Zhi D. Characteristics of ginsenoside Rd-induced effects on rat intestinal contractility with irritable bowel syndrome. Nat Prod Res 2023; 37: 3152-3157.

[37] Zheng C, Zhong Y, Zhang W, Wang Z, Xiao H, Zhang W, Xie J, Peng X, Luo J and Xu W. Chlorogenic acid ameliorates post-infectious irritable bowel syndrome by regulating extracellular vesicles of gut microbes. Adv Sci (Weinh) 2023; 10: e2302798.

[38] Xu J, Zhao X, Yang S, Tang M, Zhao R and Hu S. Chlorogenic acid and intestinal health: mechanistic insights and therapeutic applications. Food Funct 2025; 16: 4257-4277.